

Supporting Information

Evaluation of Arene Ruthenium(II) *N*-heterocyclic Carbene Complexes as Organometallics Interacting with Thiol and Selenol Containing Biomolecules

Luciano Oehninger,^a Maria Stefanopoulou,^b Hamed Alborzinia,^c Julia Schur,^a Stephanie Ludewig,^a Kazuhiko Namikawa,^d Alvaro Muñoz-Castro,^e Reinhard Köster,^d Knut Baumann,^a Stefan Wölfl,^c William S. Sheldrick,^b Ingo Ott ^{a*}

a) Institute of Medicinal and Pharmaceutical Chemistry, Technische Universität Braunschweig, Beethovenstr. 55, D-38106 Braunschweig, Germany, b) Lehrstuhl für Analytische Chemie, Ruhr-Universität Bochum, D-44780 Bochum, Germany, c) Institute of Pharmacy and Molecular Biotechnology, Ruprecht-Karls-Universität Heidelberg, Im Neuenheimer Feld 364, D-69120 Heidelberg, Germany, d) Division of Cell Biology and Cell Physiology, Zoological Institute, Technische Universität Braunschweig, Spielmannstr. 8, D-38106 Braunschweig, Germany, e) Department of Chemical Sciences, Universidad Andres Bello, Republica 275, Santiago, Chile

1) Computational Chemistry

2) Stability in solution (UV-Vis spectroscopy)

3) Interaction with *N*-acetylcysteine (¹H NMR spectroscopy)

4) MS/MS spectra after incubation with peptides

5) References

1) Computational Chemistry

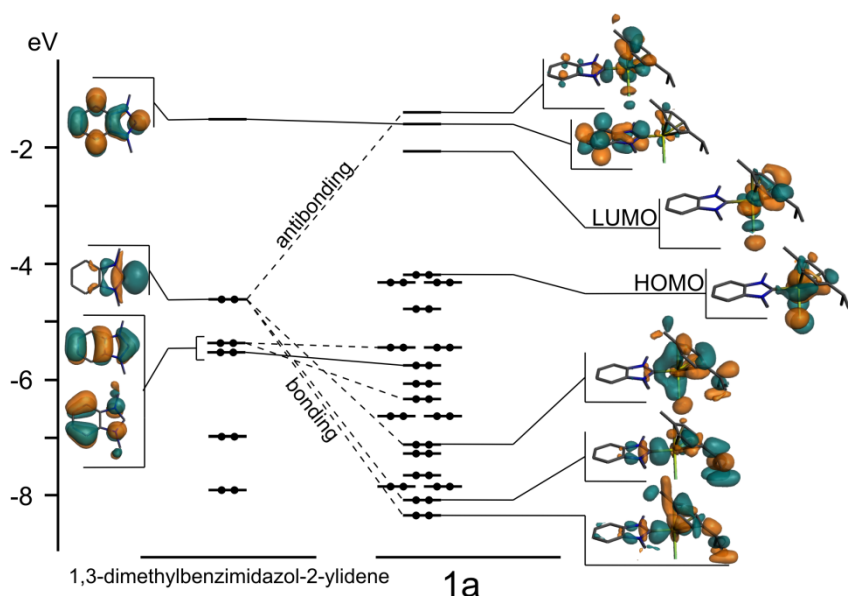


Figure S1. Molecular orbital diagram denoting the (*p*-cymene)(NHC)RuCl₂ interaction, where contribution larger than 20% to the **1a** molecular orbitals are shown. The s-donor interaction exhibits the larger bonding/antibonding gap reflecting its main role in such interaction. This diagram is representative and can be extended to **2a**, **3a** and **4a**.

	1a	2a	3a	4a
Distances (Å)				
Ru-NHC	2.061	2.062	2.090	2.063
Ru(η^6 - <i>p</i> -cymene)	1.796	1.797	1.769	1.796
Ru-Cl	2.451	2.455	2.457	2.458
BDE (kcal/mol)				
Ru-NHC	61.34	64.01	59.46	62.54
Ru(η^6 - <i>p</i> -cymene)	58.44	56.46	57.61	59.36
Ru-Cl (each)	126.58	125.15	124.72	124.90
Pop. Analysis				
Ru(II)	+0.475	+0.478	+0.474	+0.467
NHC	+0.343	+0.349	+0.333	+0.314
<i>p</i> -cymene	+0.183	+0.172	+0.188	+0.214
[2Cl] ²⁻	-1.001	-0.999	-0.995	-0.995

Table S1. Selected distances, bond dissociation energies and population analysis for **1a** - **4a**

Theoretical considerations concerning hydrolysis

Compounds **1a** - **4a** in aqueous medium can undergo hydrolysis leading to a ligand exchange involving the chlorido ligands to form the respective aquo-complexes, namely $[(p\text{-cymene})\text{RuCl}(\text{H}_2\text{O})(\text{NHC})]^+$, and $[(p\text{-cymene})(\text{NHC})\text{Ru}(\text{H}_2\text{O})_2]^{2+}$, where the structures vary slightly from the chlorido counterparts (see table S2 and figures S2, S3). Interestingly, a similar theoretical evaluation of the BDE for the involved arene and NHC ligand in the aquo-complexes reveals an enhanced bonding strength amounting to values in the 71 - 99 kcal/mol range for both organometallic fragments driven by the difference in the Cl^- and H_2O ligands. The latter point suggests that the $\text{Ru}(\eta^6\text{-}p\text{-cymene})$ or Ru-NHC interaction can be modulated by the presence of different ligands into the coordination sphere of Ru(II), becoming more labile under the presence of ligands with stronger interaction towards the ruthenium center.

$[(p\text{-cymene})\text{Ru}(\text{H}_2\text{O})_2(\text{NHC})]^{2+}$	1a'	2a'	3a'	4a'
Distances (\AA)				
Ru-NHC	2.037	2.041	2.041	2.052
$\text{Ru}(\eta^6\text{-}p\text{-cymene})$	1.714	1.706	1.714	1.700
Ru-OH ₂	2.161	2.176	2.157	2.170
BDE (kcal/mol)				
Ru-NHC	85.46	85.89	88.27	98.96
$\text{Ru}(\eta^6\text{-}p\text{-cymene})$	96.77	91.36	89.43	84.20
Ru-OH ₂ (each)	23.79	21.69	22.12	25.03

$[(p\text{-cymene})\text{RuCl}(\text{H}_2\text{O})(\text{NHC})]^+$	1a''	2a''	3a''	4a''
Distances (\AA)				
Ru-NHC	2.070	2.084	2.105	2.078
$\text{Ru}(\eta^6\text{-}p\text{-cymene})$	1.807	1.750	1.795	1.803
Ru-OH ₂	2.272	2.275	2.271	2.276
Ru-Cl	2.451	2.455	2.451	2.441
BDE (kcal/mol)				
Ru-NHC	73.13	72.96	71.46	75.72
$\text{Ru}(\eta^6\text{-}p\text{-cymene})$	78.69	77.04	76.47	77.87
Ru-OH ₂	20.01	20.09	19.51	19.57
Ru-Cl	216.47*	213.68*	212.37*	209.04*

Table S2. Selected distances, bond dissociation energies for the di-aquo and mono-aquo complexes derived from **1a** - **4a**, namely **1a'** - **4a'** and **1a''** - **4a''** respectively.

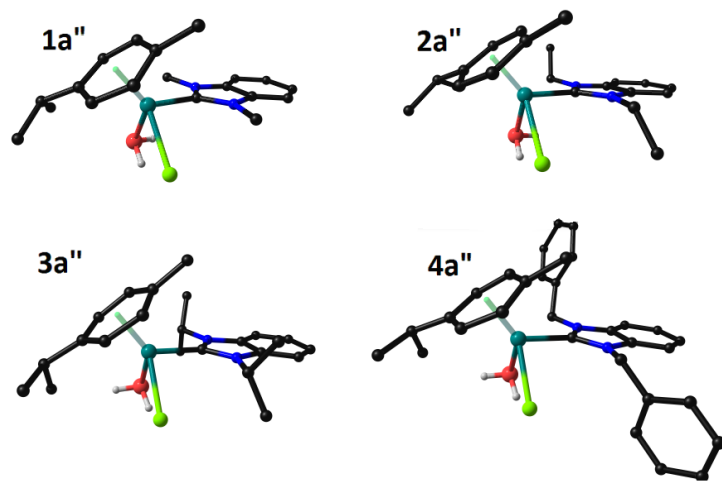


Fig S2: Optimized structures (minimum energy conformation) of the mono-aquo counterparts of **1a- 4a**

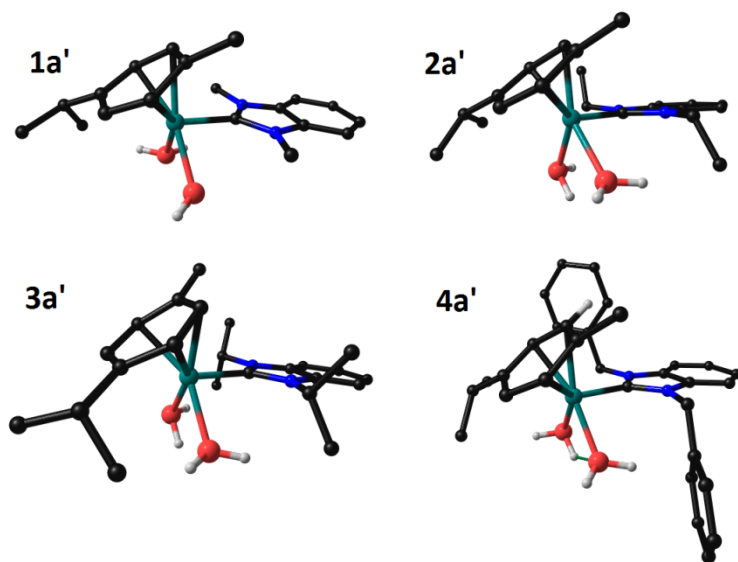


Fig S3: Optimized structures of the di-aquo counterparts of **1a- 4a**

2) Stability in Solution (UV-Vis spectroscopy)

Complex **4a** was dissolved in a 0.5% solution of acetonitrile in water and its UV-Vis spectra were monitored for 10 hours showing no changes in shape and absorption (figure S4). The spectrum of the ligand **4** shows an absorption band between 235 and 295 nm, while for complex **4a** a band is observed at 230 nm and another more intense between 280 and 300 nm corresponding to a LLCT. Due to these spectral differences between it is possible to distinguish between the free ligand **4** and the ruthenium complex **4a**. Exchange of the chlorido ligands from ruthenium arene complexes by water molecules has been reported in the literature.^{1,2} This would involve spectral changes in the range of 300-350 nm. However, in the case of **4a** this wavelength range shows absorbances of the respective NHC ligand, which hamper an evaluation of possible Cl⁻/ water exchanges by this technique.

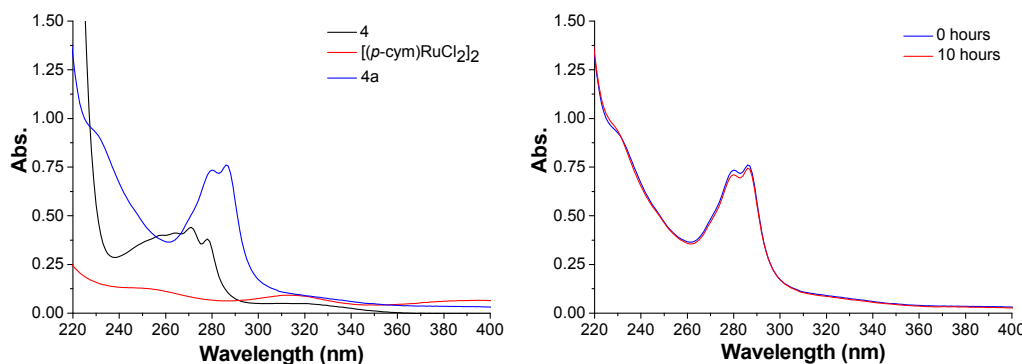


Figure S4. (right) UV-Vis spectra of ligand **4**, complex **4a** and $[(p\text{-cym})\text{RuCl}_2]_2$ in a 0.5% acetonitrile solution in H_2O ; (left) UV-Vis spectra of complex **4a** at time 0 and after 10 hours in a 0.5% acetonitrile solution in H_2O .

3) Interaction with *N*-acetylcysteine (^1H NMR spectroscopy)

Complex **1a** was incubated with *N*-acetylcysteine in $\text{DMSO}-d_6$ over 24 hours and ^1H NMR spectra were measured. For assigning the structural changes spectra of *N*-acetylcysteine, **1** 3 and **1a** in $\text{DMSO}-d_6$ were measured. The spectrum of *N*-acetylcysteine is shown in figure S5, the spectra of **1** and **1a** (see figure S6) were evaluated as follows:

1: ^1H NMR ($\text{DMSO}-d_6$): (ppm) 9.64 (s, 1H, $\text{N}-\text{CH}-\text{N}$), 8.02 (dd, 2H, $^3J_{HH}=3.2$ Hz, $^3J_{HH}=6.3$ Hz, $\text{ArH}_{5/6}$), 7.71 (dd, 2H, $^3J_{HH}=3.2$ Hz, $^3J_{HH}=6.3$ Hz, $\text{ArH}_{4/7}$), 4.08 (s, 6H, $-\text{NCH}_3$).

1a: ^1H NMR ($\text{DMSO}-d_6$): (ppm) 7.81 - 7.72 (m, 2H, C_6H_4), 7.50 - 7.43 (m, 2H, C_6H_4), 6.45 (d, 1H, MeC_6H_4-), 6.29 (d, 1H, MeC_6H_4-), 6.18 (m, 2H, MeC_6H_4-), 4.10 (s, 6H, $-\text{NCH}_3$), 3.34 (hept, 1H, CHMe_2 , $^3J_{HH}=7.0$ Hz), 2.07 (s, 3H, $\text{C}_6\text{H}_4\text{CH}_3$), 1.13 (d, 6H, $(\text{CH}_3)_2\text{CHC}_6\text{H}_4-$, $^3J_{HH}=7.0$ Hz).

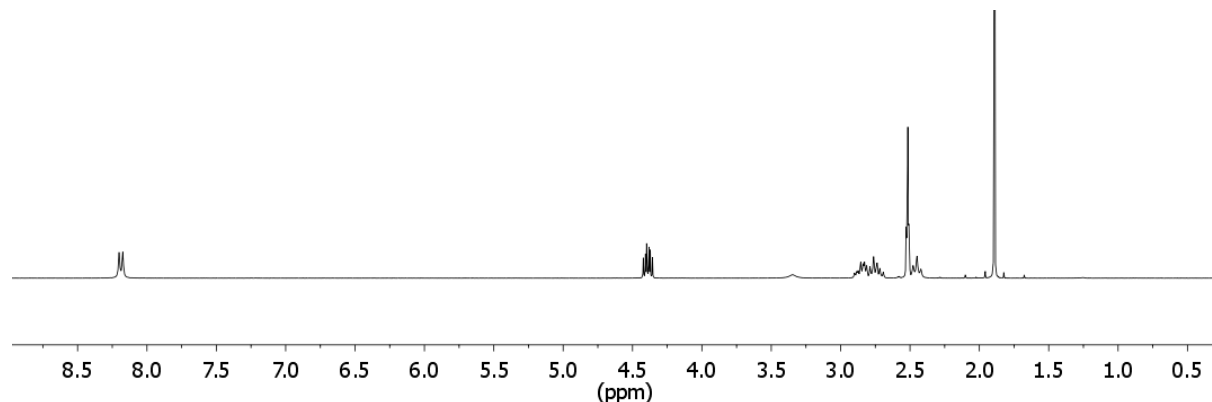


Figure S5 ^1H NMR spectrum of *N*-acetylcysteine in $\text{DMSO}-d_6$.

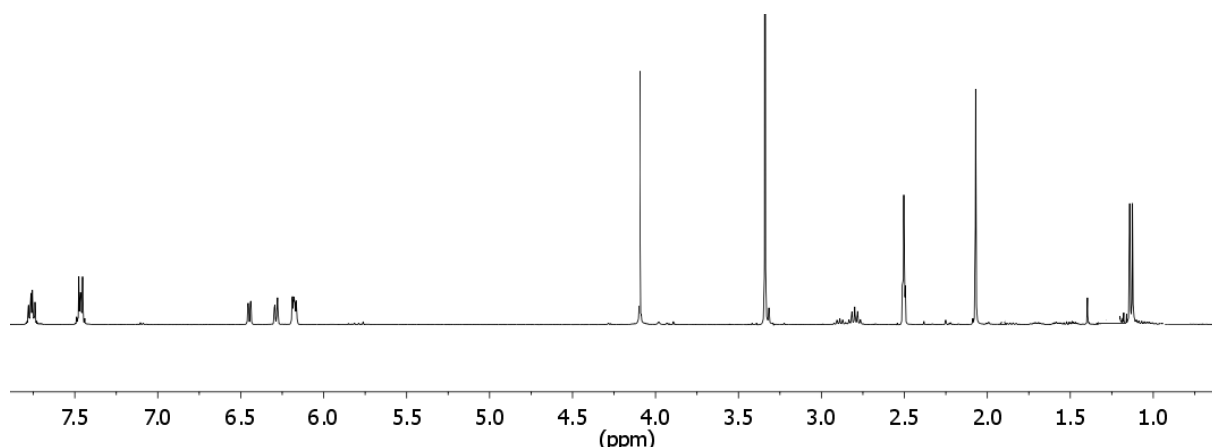


Figure S6 ^1H NMR spectrum of compound **1a** in $\text{DMSO}-d_6$

Upon exposure of the mixture of **1a** and *N*-acetylcysteine the following spectral changes were noted after 24 h (see figure S7 for the spectra after 5 min and 24 hours):

A signal at 9.62 emerged, which corresponds to the protonated C^2 of the released NHC ligand. The aromatic signals of the benzimidazolylidene core were shifted to 8.00 and 7.71 ppm and the singulett of the NCH_3 fragment moved slightly to 4.08 confirming the release of **1** from **1a**. The aromatic signals of the p-cymene ligand in the region of 6.1 - 6.5 ppm merged to a signal at 7.10 ppm. *N*-acetylcysteine was added in excess and resulted in additional emerging signals at 8.86 and 8.34 ppm (NH), 4.47 ppm (CH), 2.8-3.2 ppm (CH_2), as well as 1.96 and 1.86 (CH_3) indicating the formation of chelate complexes with ruthenium.

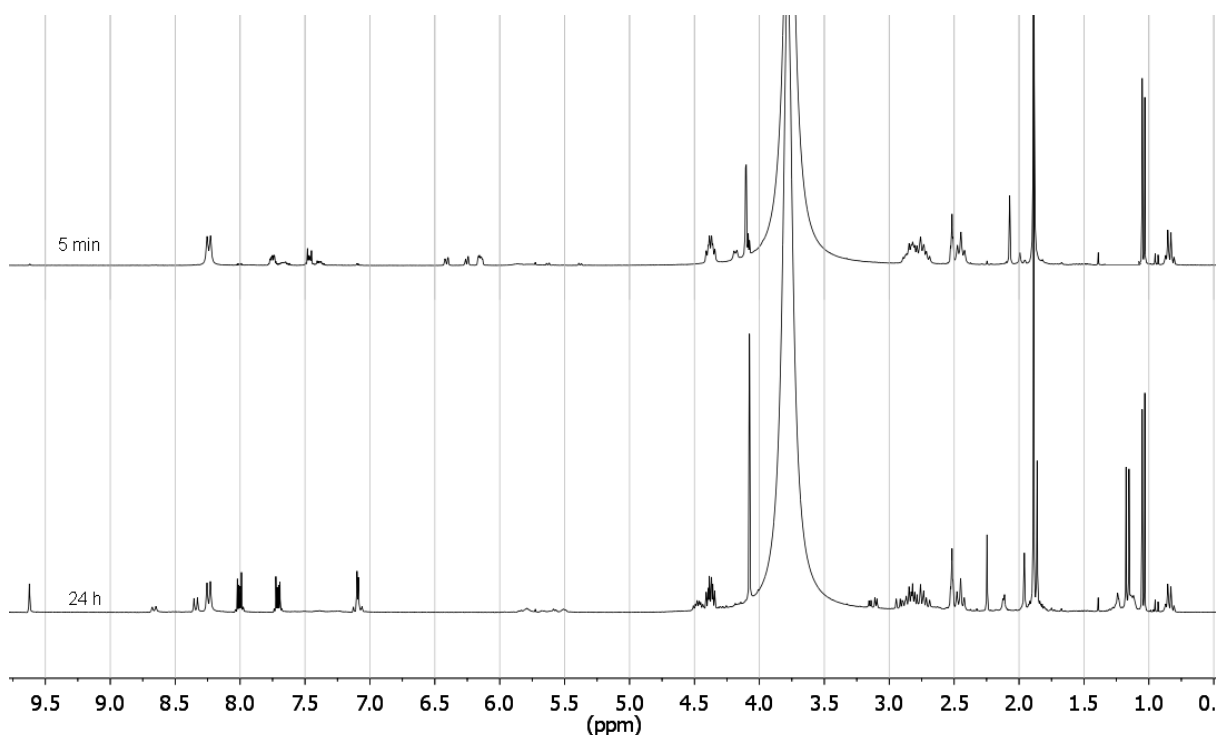


Figure S7 ^1H NMR spectrum of compound **1a** and *N*-acetyl-L-cysteine in $\text{DMSO}-d_6$ after 5 minutes and 24 hours.

3) MS/MS spectra after incubation with peptides

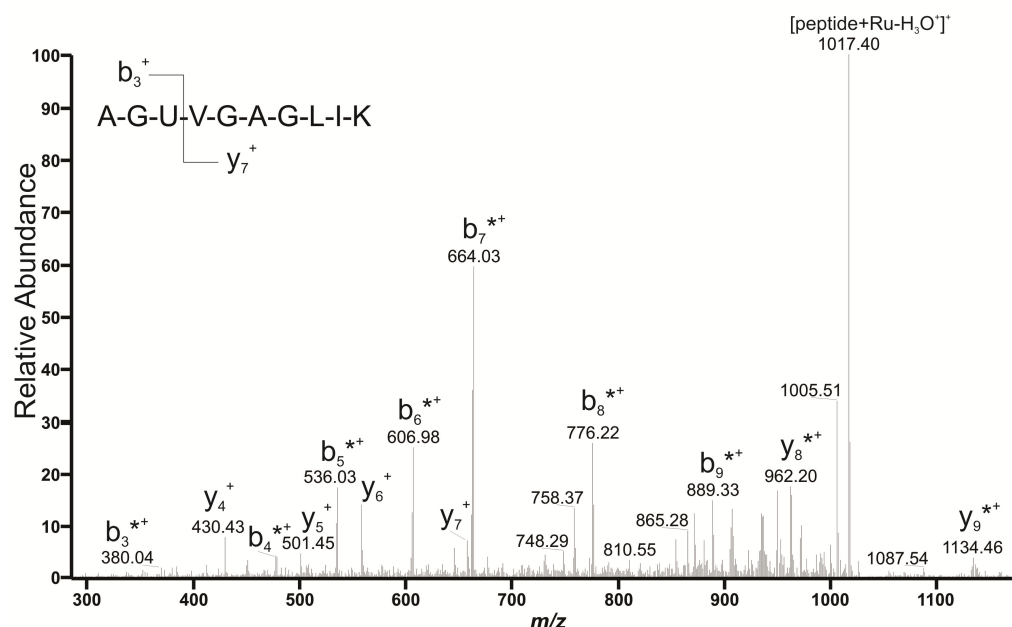


Figure S8: MS/MS spectrum of the molecular ion $[\text{peptide} + \text{Ru}]^+$ at m/z 1036 after a 4 h incubation at 37 °C of a 5:1 mixture of complex **4a** with the peptide H-AGUVGAGLIK-OH. The asterisk (*) represents the ruthenium atom.

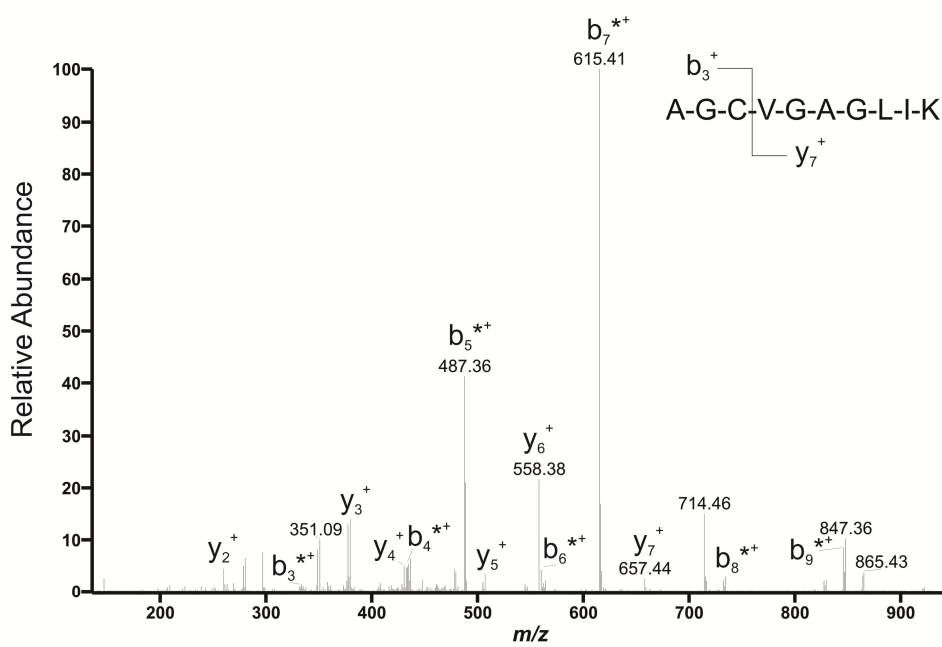


Figure S9: MS/MS spectrum of the molecular ion $[\text{peptide} + \text{Ru}]^{2+}$ at m/z 497 after a 1 h incubation at 37 °C of a 5:1 mixture of complex **1a** with the peptide H-AGCVGAGLIK-OH. The asterisk (*) represents the ruthenium atom.

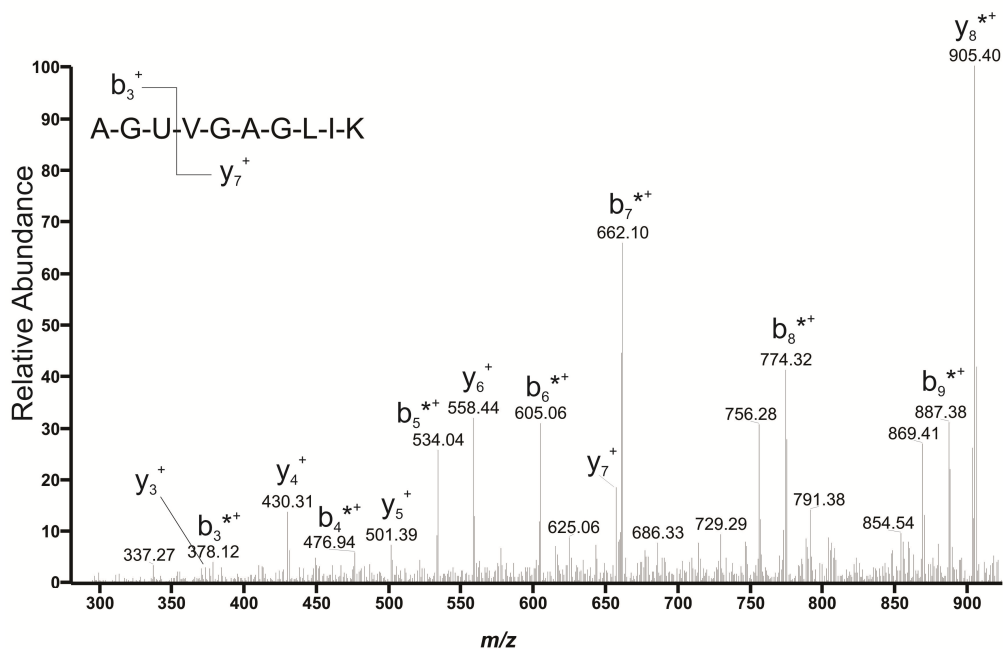


Figure S10: MS/MS spectrum of the molecular ion $[\text{peptide} + \text{Ru}]^+$ at m/z 1034 after a 1 h incubation at 37 °C of a 5:1 mixture of complex **1a** with the peptide H-AGUVGAGLIK-OH. The asterisk (*) represents the ruthenium atom.

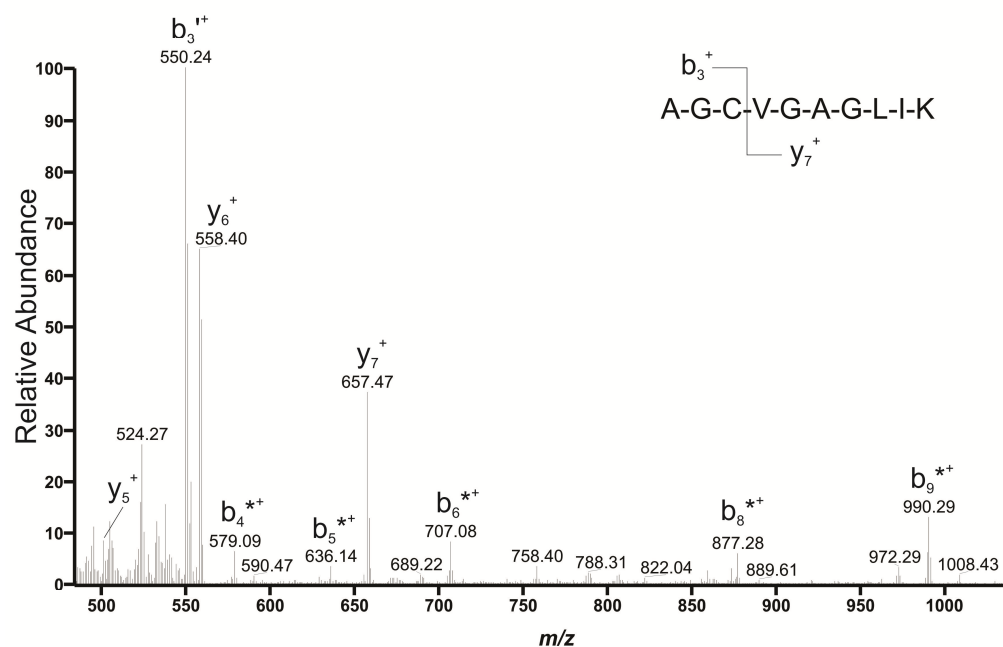


Figure S11: MS/MS spectrum of the molecular ion $[\text{peptide} + \mathbf{1a}^*]^2+$ at m/z 569 after a 1 h incubation at 37 °C of a 1:1 mixture of complex **1a** with the peptide H-AGCVGAGLIK-OH. The asterisk (*) represents the fragment ion $[\mathbf{1a} - (\text{p-cymene}) - 2\text{Cl}]^+$. Only the b_3 -ion is differentially indicated since it could be characterized as $[\mathbf{b}_3 + \mathbf{1a} - (\text{p-cymene})]^+$.

5. References (1) Morris, R. E.; et al. *J. Med. Chem.* **2001**, *44*, 3616–3621. (2) Scolaro, C. et al. *J. Inorg. Biochem.* **2008**, *102*, 1743–1748. (3) Rubbiani, R. et al. *J. Med. Chem.* **2010**, *53*, 8608–8618.

